NUMERICAL METHOD OF SOLUTION OF IRROTATIONAL FLOW OVER A SPILLWAY

POST GRADUATE OFFI...
Sub... on. 8/6/70

A Thesis Submitted
In Partial Fulfilment of the Requirements
For the Degree of
MASTER OF TECHNOLOGY

JUNE '13

by
SHAILENDRA KISHORE SHARAN

Thesis
CE-1970-M-SHA-N

to the
Department of Civil Engineering
INDIAN INSTITUTE OF TECHNOLOGY KANPUR
June 1970

To

my Grandparents

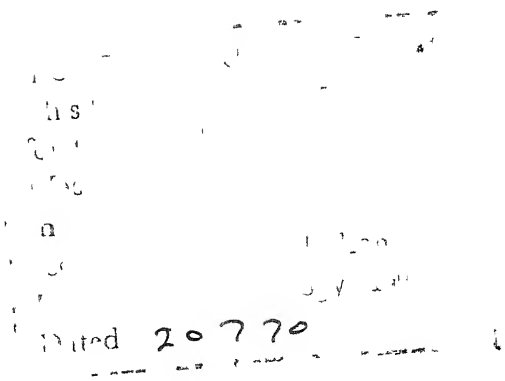

CERTIFICATE

Certified that this work, "Numerical Method of Solution of Irrotational Flow Over a Spillway" by S.K. Sharan, has been carried out under my supervision and that this work has not been submitted elsewhere for a degree.

S Surya Rao

Dr. S. Surya Rao
Assistant Professor
Department of Civil Engineering
Indian Institute of Technology
Kanpur

June, 1970

ACKNOWLEDGEMENT

I wish to express deep sense of gratitude to Dr. S. Surya Rao for his valuable guidance and constant encouragement throughout the course of this work.

I am indebted to my friends Mr. S. C. Awasthy and Mr. A. P. Chincholikar for extending their helps in many intangible ways.

Thanks are due to my other friends and colleagues but for whose help the completion of this work would have been difficult.

Shailendra Kishore Sharan

LIST OF CONTENTS

LIST OF FIGURES

NOMENCLATURE

A = a coefficient used to denote the mapping function as $W = - A . Z^2$ to represent flow in the corner

C_d = $q / (\frac{2}{3} . \sqrt{2g} . h^{1.5})$ = discharge coefficient

D = diameter of the circular crest or a parameter assumed to describe spillway shape

g = gravitational acceleration

H = total head

h = head over the spillway

k = boundary roughness scale

N_s = number of stream-lines

n = number of stream-tubes into which the bigger mesh near the corner is subdivided

l = height of the spillway

p = pressure at any point

q = discharge per unit width

u = velocity component in the x-direction

v = velocity component in the y-direction

V = complex velocity

W = complex potential

x, y = Cartesian coordinates

Z = complex variable

γ = unit weight

θ = angle of inclination of the velocity vector with x-direction

μ = dynamic viscosity

ρ = density

σ = surface tension

ϕ = velocity potential

ψ = stream function

ABSTRACT

The numerical method of solution of irrotational flow over a spillway, as developed by Cassidy, was found to be ambiguous and was not found to converge.

The method of solution developed by Cassidy was studied in detail, some of the discrepancies were rectified, and a workable method of solution has been developed. The method developed involves trial and error as well as successive approximations. Formulation of algorithms for the correction of assumed free surface and assumed value of coefficient of discharge and refinement of existing method are the main concern of this report.

The coefficient of discharge, free-surface profile, and the velocity and the pressure distributions for any given head over a given spillway could be obtained by the method that has been explained in detail in the thesis.

CHAPTER 1

INTRODUCTION

Spillway performance under varied operating conditions is of utmost importance for spillway designers. It is well known that when an ogee spillway is operated at heads higher than the design head, pressures lower than atmospheric are developed on the surface of the spillway and the coefficient of discharge increases upto a certain value of the ratio of actual head to the design head, beyond which separation occurs and the coefficient of discharge decreases rapidly (1). This characteristic is taken to advantage by spillway designers. Spillway profile is designed for heads less than maximum head so that at maximum head a higher coefficient of discharge can be obtained. This results in a shorter spillway for a certain height of the spillway or a higher spillway for a certain length of the spillway as compared to what would have been obtained by taking the maximum head as the design head. The important criterion of the design, however, is to check that cavitation does not occur due to the development of negative pressure.

In order to adopt the above mentioned rational design procedure, it is essential to investigate the flow-characteristics for spillways at heads other than design head to determine

the variation of the coefficient of discharge and minimum pressure developed on the spillway with the ratio of actual head to a reference head (2).

The flow over a spillway is of highly contracting nature and such flow can be assumed to be irrotational as long as there is no separation. Such a flow-problem is well-suited to analysis by the technique of potential theory and the results thus obtained would be very near to the actual flow over the prototype structure.

Solution of free-surface was first performed by A.Lauck in 1925 for the case of Sharp Crested weirs of infinite height by successive approximation in the complex potential plane (3). Using a pair of integral equations derived from the real and imaginary parts of Cauchy's integral formula, together with the integrated form of Bernoulli equation it was possible to obtain a new distribution of the free-surface on the basis of an assumed distribution. The process was one of successive approximation. It was found that the results converged for only a particular value of discharge.

R.V. Southwell solved the problem for a flow-region bounded by horizontal floor and free-surface by solving the Laplace equation (4). The method required adjustment of the assumed free-surface by trial and error and the relaxation solution was performed for each trial until the free-surface satisfied Bernoulli equation.

In 1964 Strelkoff published a paper on solution of highly curvilinear gravity flows (5) but the method suggested by him is restricted to straight solid boundaries only. He solved the flow over sharp crested weir of finite height by the use of conformal mapping technique. An algorithm for correction of total head was formulated by him.

G. Watters and R.L. Street solved for the free-surface profile over steps and curved humps (6). They solved the integral equation by expressing the complex velocity as infinite series. In neither Strelkoff's method nor that of Watter and Street there is any provision of specifying independently the shape of the solid boundary.

Recently a method was developed by J.J. Cassidy for the computation of coefficient of discharge, free-surface profile, pressure distribution, etc. for flow over spillways of finite height (7). A free-surface is assumed initially and by an iterative procedure for satisfying the various pertinent equations and boundary conditions, the solution is obtained. An algorithm was obtained to correct the assumed value of the coefficient of discharge through the observation of behavior of the free-surface profile from iteration to iteration. Cassidy claims this method to be one of successive approximations and according to him it is superior to other methods involving trial and error procedure. It appears that according to Cassidy, irrespective of the

free-surface assumed initially, the solution converges provided the discharge coefficient is correct. It has been found from the present study that the convergence or divergence of the solution, obtained by using the method suggested by Cassidy, depends on the initially assumed free-surface as well as the discharge coefficient.

The present study was originally intended to apply Cassidy's method for solving the problem of flow over ogee spillways with various ratios of design head to the height of the spillway. But the available time was spent in applying the method only to the case of flow over a spillway with circular crest, discovering in this process the drawbacks in Cassidy's method and developing a method of solution. The various alternative ways for the computation of the different parameters in the procedure suggested by Cassidy have been analysed and discussed and a suitable method of solution has been developed.

CHAPTER 2

ANALYSIS OF THE PROBLEM

2.1 Physical Analysis:

If the flow approaching the spillway is assumed to be subcritical, i.e. if the Froude Number of the approaching flow is less than unity, the control section for the flow is at the spillway. Under such conditions the pertinent variables that describe the discharge over a two-dimensional spillway and the free-surface profile may be grouped as shown below:

$$q = f_1(D, P, h, k, \gamma, \rho, \mu, \sigma) \quad \ldots(1)$$

$$y_o = f_2(x_o, D, P, h, k, \gamma, \rho, \mu, \sigma) \quad \ldots(2)$$

$$\phi, \psi, p, V, \theta = f_{3,4,5,6,7}(x, y, D, P, h, k, \gamma, \rho, \mu, \sigma) \quad (3)$$

wherein ϕ and ψ are the two-dimensional velocity potential and stream function, respectively. x and y are the coordinates of any point. x_o and y_o stand for the x and y coordinates of free-surface. V and θ refer to the magnitude and inclination of the velocity vector with reference to x - direction. p represents pressure at any point. The parameter D describes the shape of the spillway. P is the height of the spillway and h is the head over the spillway crest. k is the boundary roughness characteristic, γ, ρ, μ and σ

are specific weight, density, dynamic viscosity and surface tension of the fluid, respectively. g is the gravitational acceleration.

ϕ and Ψ are assumed to be zero at the stagnation point B (Fig. 1). For the solid boundary which is also a stream line, U is assumed to be zero and for the free-surface Ψ is equal to the discharge q per unit width. The two equipotential lines on the upstream and downstream ends of the flow region are assumed to form the upstream and downstream boundaries of flow region under consideration and the stream lines are considered to be straight and parallel to the solid boundary at all points along these equipotential lines.

x refers to the horizontal distance from the stagnation point B and is measured positive downstream. y denotes the vertical distance from the stagnation point B and is measured positive upwards. The parameter D is assumed to describe the shape of the spillway completely. This type of single-parameter is not obtained for all shapes of spillways. In the case of standard spillway this parameter is the design head and in the case of circular crest spillway this may be taken as the diameter of the circular-crest. In the present analysis D is assumed to be a length parameter.

Using π -theorem the following relationships may be obtained.

$$\frac{q}{\sqrt{2g}\ h^{3/2}} = f_8\left(\frac{P}{D}, \frac{h}{D}, \frac{k}{D}, \frac{q D \rho}{(P+h)\mu}, \frac{q}{(P+h)\sqrt{(\sigma/\rho D)}}\right) \quad \ldots(4)$$

$$\frac{y_o}{D} = f_9 \left(\frac{x_o}{D}, \frac{P}{D}, \frac{h}{D}, \frac{k}{D}, \frac{q\,D\rho}{(P+h)\mu}, \frac{q}{(P+h)\sqrt{(\sigma/\rho\,D)}}\right) \quad (5)$$

$$\frac{\phi}{\sqrt{2g}\,D^{3/2}}, \frac{\psi}{\sqrt{2g}\,D^{3/2}}, \frac{P}{D}, \frac{V}{\sqrt{2gD}}, \theta =$$

$$= f_{10,11,12,13,14}\left(\frac{x}{D}, \frac{y}{D}, \frac{P}{D}, \frac{h}{D}, \frac{k}{D}, \frac{q\,D\rho}{(P+h)\mu}, \right.$$

$$\left.\frac{q}{(P+h)\sqrt{(\sigma/\rho\,D)}}\right) \quad \ldots (6)$$

The discharge and the free-surface profile are thus functions of the relative height of spillway P/D, the relative head over the spillway h/D, the relative roughness k/D, a Reynolds number and a Weber number.

If, on the other hand the Froude number of the approaching flow is greater than unity and the spillway height is low enough to prevent the formation of a surge, the control section is upstream from the spillway and the discharge coefficient for a given head is automatically determined by the Froude number which is an independent variable under this condition. In such case, the discharge coefficient is independent of the profile of spillway. The analysis reported herein is restricted to that for the subcritical approaching flow.

It has been found that the effect of boundary layer on the free-surface profile and the coefficient of discharge can be neglected (7). Hence the Reynolds number and the relative roughness may be dropped from eqn.(6). In addition; Weber number may be dropped if the analysis is –

restricted to large-scales where the surface tension has insignificant role. Hence, equations 4, 5 and 6 are simplified to,

$$\frac{q}{\sqrt{2g}\, h^{3/2}} = f_{15}\left(\frac{P}{D}, \frac{h}{D}\right) \qquad \ldots(7)$$

$$\frac{y_o}{D} = f_{16}\left(\frac{x_o}{D}, \frac{P}{D}, \frac{h}{D}\right) \qquad \ldots(8)$$

$$\frac{\phi}{\sqrt{2g}\, D^{3/2}}, \frac{\psi}{\sqrt{2g}\, D^{3/2}}, \frac{p}{D}, \frac{V}{\sqrt{2gD}}, \theta$$

$$= f_{17,18,19,20,21}\left(\frac{x}{D}, \frac{y}{D}, \frac{P}{D}, \frac{h}{D}\right) \ldots(9)$$

2.2 Mathematical Analysis

As the flow is highly contracting and over a spillway with a streamlined profile, it may be assumed to be irrotational and so potential theory may be used for the solution of the problem (11).

It is found to be simpler to work in the complex-potential plane. When the region between the solid boundary and the free-surface is mapped in the complex-potential plane, the physical picture shown in Fig. 1 will be transformed to a simple rectangular configuration as shown in Fig. 2. In the complex-potential plane the velocity potential ϕ is represented as abscissa and stream function ψ as the ordinate. The complex potential W is represented as

$$W = \phi + i\psi \qquad \ldots(10)$$

As W is analytic,

$$\frac{dW}{dZ} = \frac{\partial\phi}{\partial x} + i\frac{\partial\psi}{\partial x}$$

$$= \frac{\partial\psi}{\partial y} - i\frac{\partial\phi}{\partial y} \qquad \ldots(11)$$

Z refers to the complex physical plane and is represented as

$$Z = x + iy \qquad \ldots(12)$$

By the definition of ϕ and ψ ,

$$u = \frac{\partial\phi}{\partial x} = \frac{\partial\psi}{\partial y} \qquad \ldots(13)$$

$$v = \frac{\partial\phi}{\partial y} = -\frac{\partial\psi}{\partial x} \qquad \ldots(14)$$

Substituting this in Eqn. 11,

$$\frac{dW}{dZ} = \frac{\partial\phi}{\partial x} + i\frac{\partial\psi}{\partial x}$$

$$= u - iv \qquad \ldots(15)$$

in which u is the horizontal component and v is the vertical component of the velocity so that,

$$u = V \cos\theta$$

$$v = V \sin\theta \qquad \ldots(16)$$

Thus,

$$\frac{dW}{dZ} = u - \imath v$$

$$= V \cos \theta - \imath V \sin \theta$$

$$= V (\cos \theta - \imath \sin \theta)$$

$$= V e^{-\imath\theta} \qquad \ldots(17)$$

Taking natural logarithm of the quantities on both sides of Eqn. 17,

$$\ln \left(\frac{dW}{dZ}\right) = \ln V - i\theta \qquad \ldots(18)$$

Now ln (dW/dZ) is analytic, so its real and imaginary parts ln V and θ must satisfy the Cauchy-Riemann equation and Laplace equation.

Hence, by Laplace equation

$$\frac{\partial^2 \ln (V)}{\partial \psi^2} + \frac{\partial^2 \ln (V)}{\partial \phi^2} = 0 \qquad \ldots(19)$$

$$\frac{\partial^2 \theta}{\partial \psi^2} + \frac{\partial^2 \theta}{\partial \phi^2} = 0 \qquad \ldots(20)$$

and by Cauchy-Riemann eqn.,

$$\frac{\partial \ln (V)}{\partial \phi} = \frac{\partial(-\theta)}{\partial \psi} = -\frac{\partial \theta}{\partial \psi} \qquad \ldots(21)$$

$$\frac{\partial \ln (V)}{\partial \psi} = -\frac{\partial(-\theta)}{\partial \phi} = \frac{\partial \theta}{\partial \phi} \qquad \ldots(22)$$

The connection between complex-potential plane and physical plane is formulated by considering the expressions for the stream function and the velocity potential,

$$d\psi = \frac{\partial \psi}{\partial x}\, dx + \frac{\partial \psi}{\partial y} \cdot dy \qquad \ldots(23)$$

$$d\phi = \frac{\partial \phi}{\partial x}\, dx + \frac{\partial \phi}{\partial y} \cdot dy \qquad \ldots(24)$$

and

$$u = \frac{\partial \phi}{\partial x} = \frac{\partial \psi}{\partial y}$$

$$v = \frac{\partial \phi}{\partial y} = -\frac{\partial \psi}{\partial x}$$

Hence,

$$d\psi = -vdx + udy \qquad \ldots(25)$$

$$d\phi = udx + vdy \qquad \ldots(26)$$

Solving these two equations simultaneously,

$$dx = \frac{ud\phi - vd\psi}{u^2+v^2} \qquad \ldots(27)$$

$$dy = \frac{vd\phi - ud\psi}{u^2 + v^2} \qquad \ldots(28)$$

Substituting $u = V \cos\theta$ and $v = V \sin\theta$,

$$dx = \frac{\cos\theta}{V}\, d\phi - \frac{\sin\theta}{V}\, d\psi \qquad \ldots(29)$$

$$dy = \frac{\sin\theta}{V}\, d\phi + \frac{\cos\theta}{V}\, d\psi \qquad \ldots(30)$$

Differentiating the above two equations with respect to ϕ and ψ a set of four equations is obtained as

$$\frac{dx}{d\phi} = \frac{\cos\theta}{V} - \frac{\sin\theta}{V}\frac{d\psi}{d\phi} \qquad \ldots(31a)$$

$$\frac{dy}{d\phi} = \frac{\sin\theta}{V} + \frac{\cos\theta}{V}\frac{d\psi}{d\phi} \qquad \ldots(32a)$$

$$\frac{dx}{d\psi} = \frac{\cos\theta}{V}\frac{d\phi}{d\psi} - \frac{\sin\theta}{V} \qquad \ldots(31b)$$

$$\frac{dy}{d\psi} = \frac{\sin\theta}{V}\frac{d\phi}{d\psi} + \frac{\cos\theta}{V} \qquad \ldots(32b)$$

Expression for distances along the stream line is

$$\frac{ds}{d\phi} = \frac{1}{V} \qquad \ldots(32c)$$

Finally, for the free-surface the pressure is zero. Hence, Bernoulli equation for the free surface is reduced to the form given below:

$$\frac{V^2}{2g} + y = H \qquad \ldots(33)$$

Thus there are five independent equations out of ten equations 19 through 22, 31a, 31b, 32a, 32b, 32c and 33 to solve for the five unknowns θ, V, x, y and H for the known values of ϕ and ψ in the ϕ - ψ plane. Only two equations out of the four equations 19 through 22 and two equations out of the five equations 31a, 31b, 32a, 32b, 32c are independent.

In order to make the solution as general as possible all the variables were made dimensionless as described in the first part of this chapter. Now onwards all the variables have been used to represent their dimensionless form.

For the numerical solution the flow-region in the complex-potential plane was divided to form a grid as shown in Fig. 3. The two meshes near the stagnation point were subdivided to form still smaller meshes for the reasons mentioned later.

The following finite difference equation, derived by W.G. Bickley (8) was substituted for equation 20 as

$$20\theta_o = 4(\theta_1+\theta_2+\theta_3+\theta_4) + (\theta_5+\theta_6+\theta_7+\theta_8) \qquad \ldots(34)$$

In the above equation the subscripts denote the values corresponding to particular node point as shown in Fig. 4.

Equations 21 and 22 were represented in the integral form as,

$$\Delta \ln (V) = \int_{\phi_1}^{\phi_2} - \frac{\partial\theta}{\partial\psi}\, d\phi \qquad \ldots(35)$$

$$\Delta \ln (V) = \int_{\psi_1}^{\psi_2} \frac{\partial\theta}{\partial\phi}\, d\psi \qquad \ldots(36)$$

in which $\Delta \ln (V)$ is the difference in $\ln (V)$ over the interval of integration.

Equations 31a, 31b, 32a, 32b and 32c are represented in integral forms as

$$\Delta x = \int_{\psi_1}^{\psi_2} - \frac{\sin\theta}{V}\, d\psi \qquad \ldots(37a)$$

$$\Delta x = \int_{\phi_1}^{\phi_2} \frac{\cos\theta}{V}\, d\phi \qquad \ldots(37b)$$

$$\Delta y = \int_{\psi_1}^{\psi_2} \frac{\cos\theta}{V}\, d\psi \qquad \ldots(38a)$$

$$\Delta y = \int_{\phi_1}^{\phi_2} \frac{\sin\theta}{V}\, d\phi \qquad \ldots(38b)$$

$$\Delta s = \int_{\phi_1}^{\phi_2} \frac{1}{V}\, d\phi \qquad \ldots(38c)$$

The above equations are valid only along lines of constant ϕ or ψ.

Mapping Function for Singular Point.

At the stagnation point B a singularity exists. At this point the velocity becomes zero and hence the equations 37 and 38 for Δx, Δy or Δs cannot be used at this point. The direction of velocity vector is undefined at this point. This difficulty was avoided by using the mapping function

$$W = - A \cdot Z^2 \qquad \ldots(39)$$

near the stagnation point. The coefficient A was evaluated

by equating at point F (Fig. 5) the magnitude of velocity obtained from equations for corner flow and the outside flow. Separating the real and imaginary parts of equation (39)

$$\frac{\phi}{A} = -x^2 + y^2 \qquad \ldots(40)$$

$$\frac{\psi}{A} = -2xy \qquad \ldots(41)$$

By solving these two equations simultaneously, expressions for x and y are obtained as

$$x = -\sqrt{\frac{-\phi + \sqrt{\phi^2 + \psi^2}}{2A}} \qquad \ldots(42)$$

$$y = \sqrt{\frac{\phi + \sqrt{\phi^2 + \psi^2}}{2A}} \qquad \ldots(43)$$

Differentiating equation 41 with respect to x, along a stream line,

$$\frac{dy}{dx} = \frac{\psi}{2Ax^2} \qquad \ldots(44)$$

Hence expression for θ is obtained as

$$\theta = \tan^{-1}\left(\frac{\psi}{-\phi + \sqrt{\phi^2 + \psi^2}}\right) \qquad \ldots(45)$$

Using Eqn. 15 and differentiating W with respect to Z,

$$\frac{dW}{dZ} = -2AZ = u - iv$$

separating the real part,

$$u = -2Ax$$

substituting the expression for x obtained from Eqn. 42

$$V = \frac{u}{\cos\theta} = \frac{2A}{\cos\theta}\sqrt{\frac{-\phi + \sqrt{\phi^2 + \psi^2}}{2A}} \qquad \ldots(46)$$

Solving for A, expression for A is obtained as

$$A = \frac{(V\cos\theta)^2}{2(-\phi+\sqrt{\phi^2 + \psi^2})} \qquad \ldots(47)$$

While using Eqn. 34, the stagnation point was avoided by computing the values of θ for the points adjacent to the stagnation point by using Eqn. 45. Value of A was not needed for this computation. It was computed by Eqn. 47 after the velocity for the points adjacent to the stagnation point is known by using equation 35 and 36. To start with the computation of x and y from the origin, equations 42 and 43 were used in place of the general equations 37 and 38.

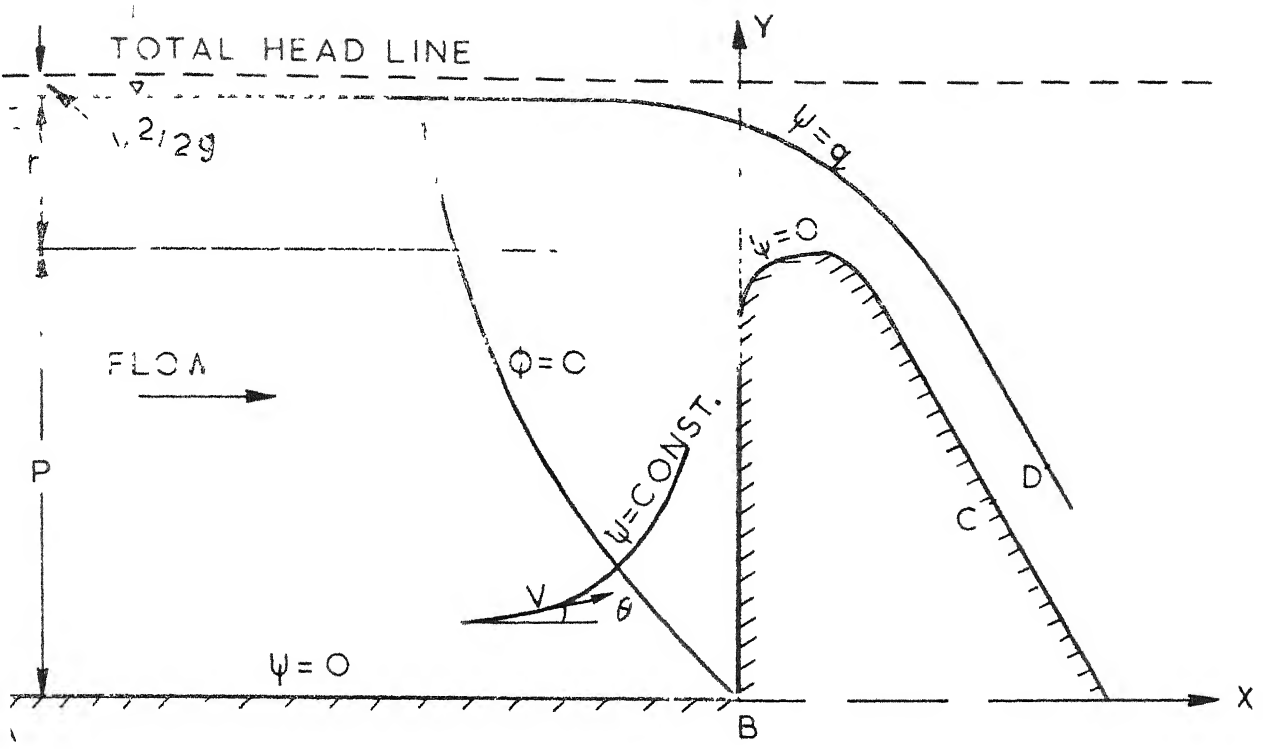

FIG 1 DEFINITION SKETCH FOR FLOW OVER SPILLWAY IN PHYSICAL PLANE

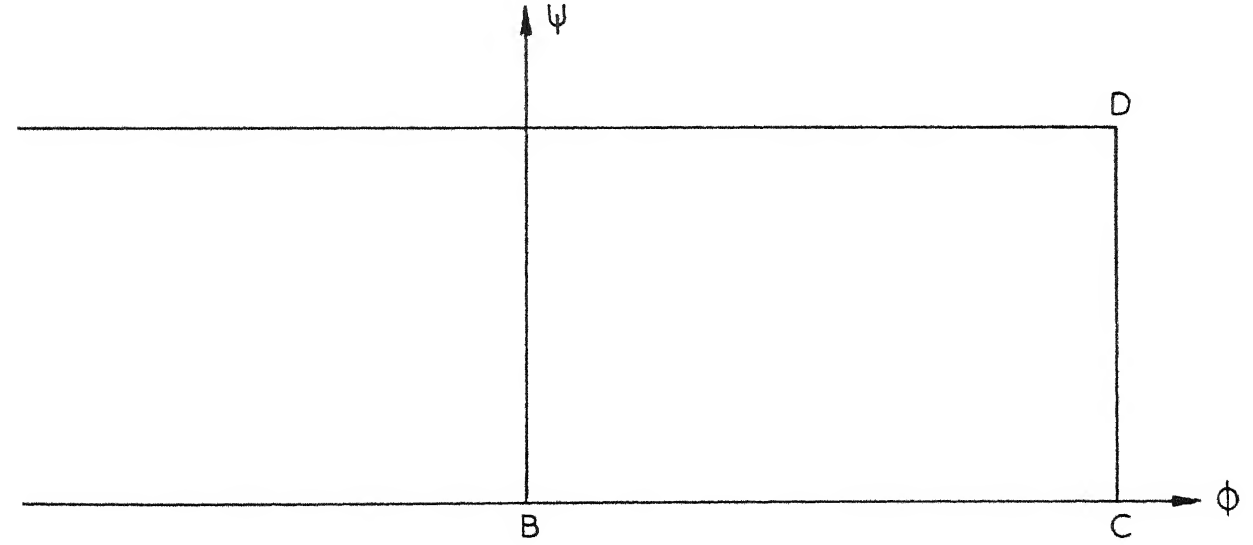

FIG 2 FLOW-REGION MAPPED INTO COMPLEX-POTENTIAL PLANE

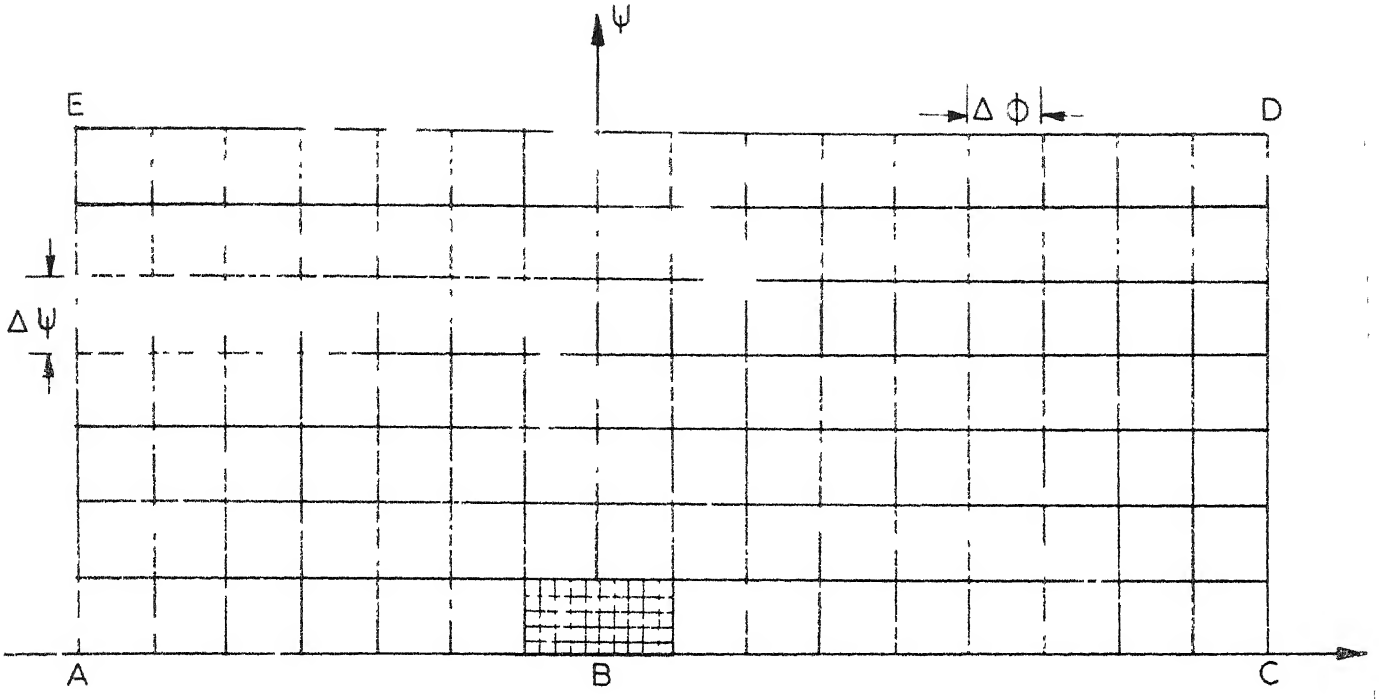

FIG 3 FINITE DIFFERENCE GRID

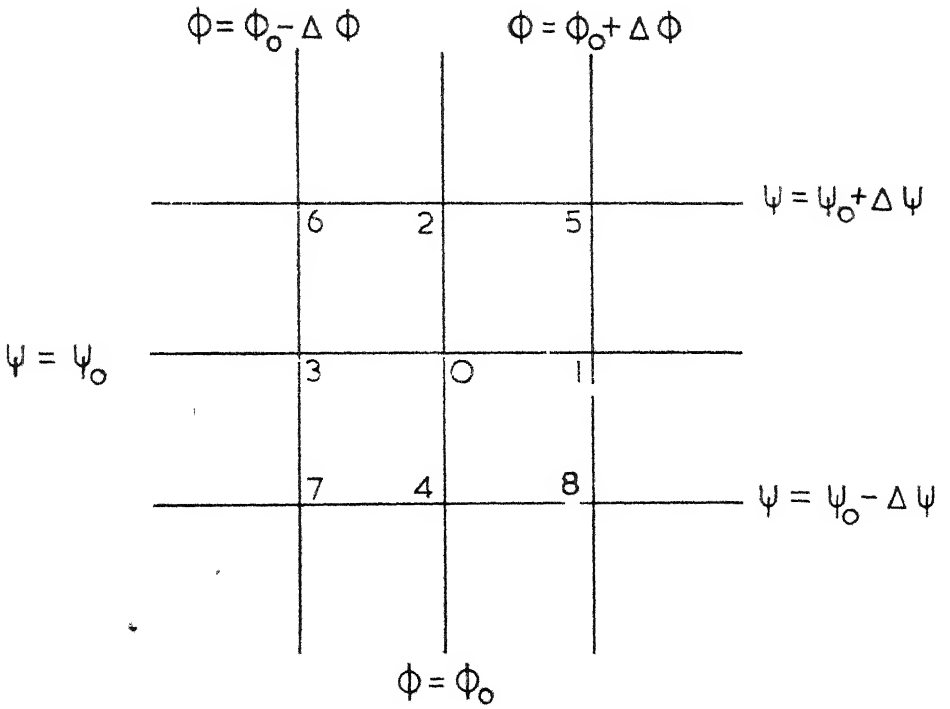

FIG. 4 FINITE DIFFERENCE MESH

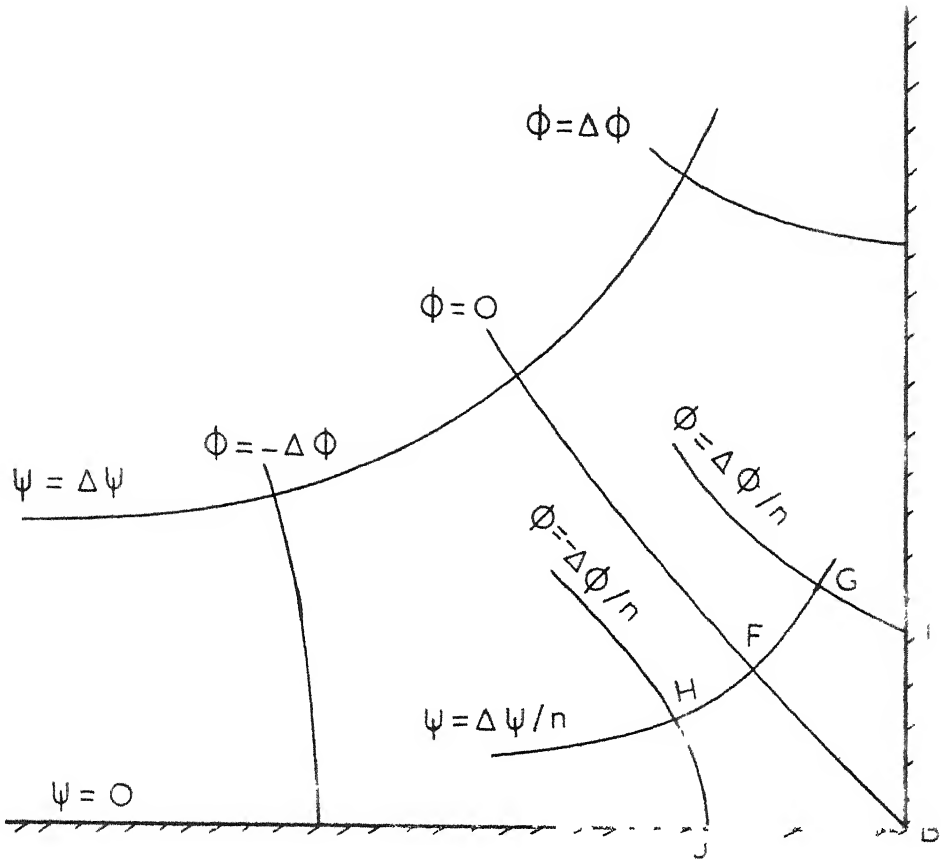

(a) PHYSICAL PLANE

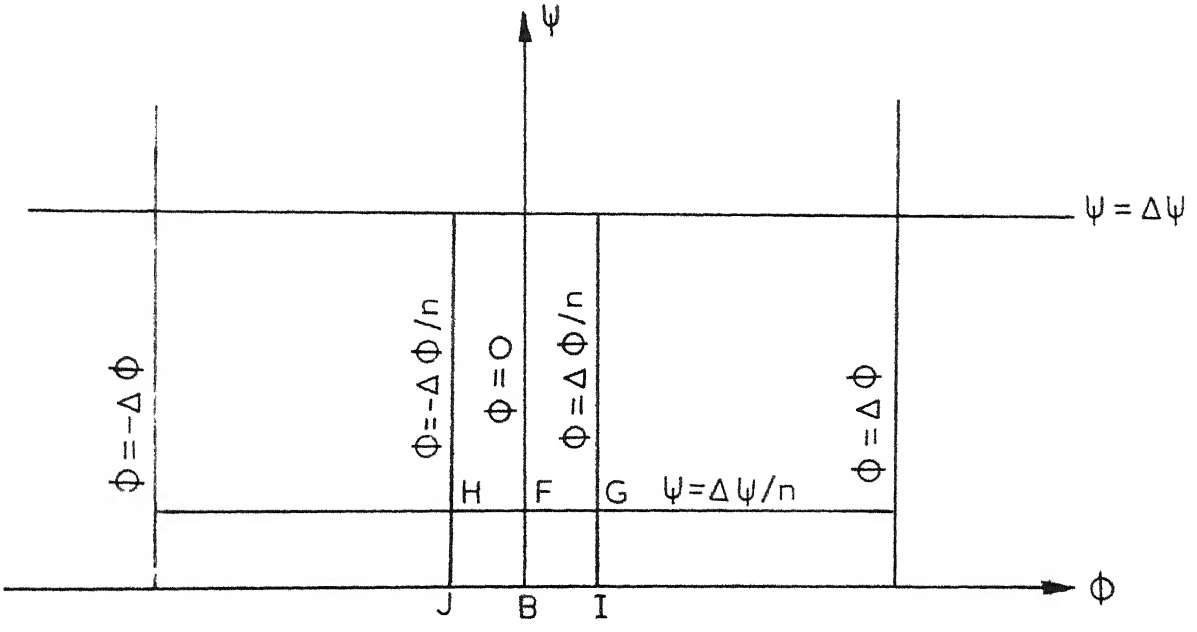

(b) COMPLEX-POTENTIAL PLANE

FIG 5 FLOW NEAR THE CORNER

CHAPTER 3

NUMERICAL SOLUTION

Numerical Method:

The main aim of the problem is to solve the equations along with pertinent boundary conditions developed in chapter 2 for obtaining the flow net and the coefficient of discharge for irrotational flow over a spillway.

Various alternative procedures to satisfy the various equations have been tried. The one found to be successful has been described in this Chapter. The behaviour of the solutions observed in the rest of the procedures studied has been discussed in chapter 4.

As stated earlier all the computations have been made in the complex-potential plane. For the given spillway shape and head over the spillway a rough free-surface was obtained by drawing a flow net for assumed free-surface profile and -

correcting the free-surface on the basis of the flow-net drawn. This was done to promote convergence.

On the basis of this rough flow-net obtained, values of θ were assumed for all the nodal points on the boundaries in the ϕ-ψ grid as shown in figure 3. By using equations derived in previous chapter it was then possible to compute all the other variables θ, V, x, y etc. for all the nodes in the complex-potential grid and thus it was possible to obtain a new distribution of θ for the boundary. This procedure was repeated for a few iterations (generally two or three) to observe the behavior of the free-surface. By observing the behavior of the free-surface obtained for a few different values of C_d, covering almost the whole range it was possible to make necessary corrections in the initial assumption of distribution of θ of free surface, if the same was in large error. Later, when the assumed free-surface was reasonably corrected, the procedure was repeated for different coefficients of discharge and the particular value of discharge coefficient for which the change of x and y coordinates of the free surface after a certain number of iterations is less than 1% of the values before the iteration was considered to be the right value.

The free surface obtained after each iteration diverged upward or downward depending upon the initial assumption of the free surface as well as the value of coefficient of discharge.

It converged to the right free-surface for a particular value of C_d only and that too when the initial assumption was not very wrong.

The algorithms obtained for correcting the C_d value and the initially assumed free-surface are discussed later in this chapter. The procedure adopted for correcting the free-surface profile on the basis of the assumed or old distribution of θ are listed below:

1. The value of discharge q was computed for the assumed value of C_d, using equation,

$$q = \frac{2}{3} C_d h^{3/2}$$

wherein all the variables should be in their dimensionless form.

2. The flow-region was divided into suitable number of stream tubes depending upon the required accuracy and available computer time. The difference $\Delta\psi$ in the values of ψ for two adjacent stream lines is given as

$$\Delta\psi = q/(N_s - 1)$$

where N_s is the number of total stream-lines chosen for computation.

For using equation 34, it was required to assume square meshes in the ϕ-ψ grid and hence the difference $\Delta\phi$ between two adjacent equipotential lines was taken as equal to $\Delta\psi$ (Fig.3). The number of equipotential lines was chosen on the basis of the

rough flow-net drawn and by assuming the positions of the upstream and downstream boundaries far enough to assume the equipotential lines to be straight lines on the two boundaries.

3. On the basis of the rough flow-net drawn, distribution of θ was assumed for the nodal points on the boundaries. For the upstream and downstream boundaries these were assumed to be constant and equal to zero and slope of the spillway at the downstream boundary respectively.

4. θ-field for the interior points in the complex potential grid was computed by successively applying equation 34 to each interior point by the relaxation procedure, until the values obtained after two consecutive iterations differed within the permissible limit.

5. Velocity distribution along the free-surface was computed such that it satisfied both equations 33 and 38b simultaneously. The computation was started from the upstream end where the velocity distribution was assumed to be uniform. For the successive points, firstly a rough value of y was assumed and by using eqn. 33, V was computed. This V was substituted in equation 38b to get a more correct value of y. Iterations for y and V were done till the two successive values were within specified limit. This was repeated for all successive points upto the downstream end.

6. The velocity distribution was known at this stage for the free-surface as computed in step 5 and along the upstream boundary by assuming uniform flow-distribution along that boundary. Hence, velocity at any interior point and along the solid boundary was computed by integrating along both the equipotential-line and stream-line separately by using equations 35 and 36 and then taking the mean of the two values of ln V.

7. x and y coordinates for all the nodes were computed by using equations 37a, 37b, 38a, 38b and 38c. Computation was started from the stagnation point, the origin. To start with, equations 42 and 43 were used to avoid the singularity at the origin.

Using equation 38c the values of $s(\phi, \psi)$ were computed for each point along the spillway profile. It was assumed to be zero at the origin and was taken positive downstream. $x(\phi,\psi)$ and $y(\phi, \psi)$ were computed along the spillway profile by using their functional relationship with $s(\phi, \psi)$ for the given profile of the spillway. With the help of eqn. 37b, $x(\phi, \psi)$ was computed along the bed upto the upstream boundary. $y(\phi,\psi)$ along the upstream boundary was known by assuming uniform flow.

$x(\phi, \psi)$ and $y(\phi, \psi)$ for the other interior points and the free surface was computed by integrating along the streamlines starting from the upstream boundary and also along the equi-potential lines starting from the solid boundary and then taking

the arithmetic mean of the two values thus obtained.

8. The behavior of the free-surface thus obtained was observed and another value of C_d was assumed accordingly. At this stage it was also decided whether a correction in the assumed θ-values for the free-surface was required or not. If it was found to be essential, the correction in the θ-distribution for the free-surface was done suitably and the procedure was cycled back to step 3. The algorithm for obtaining the rough free-surface to use as an initial assumption for correcting the value of C_d as well as obtaining a more refined free-surface by the process of successive approximation is described below.

If the negative values of θ assumed for the free-surface for any portion were too high, the free-surface in that region obtained after each iteration progressively diverged downward, i.e. $y_o(\phi, \psi)$ for the free surface decreased after each iteration for the whole range of values of C_d (Fig. 6). On the other hand if it was too low, the free-surface obtained after each iteration diverged upward, i.e. $y_o(\phi, \psi)$ for the free-surface increased progressively after each iteration for the whole range of values of C_d. On this basis it was possible to correct the assumed θ-distribution by making suitable adjustments.

After the approximately correct free-surface was obtained by the method mentioned above, the divergence in different directions, upwards or downwards was observed for the free-surface for

different values of C_d. If the value of C_d was too high, the free-surface diverged upwards and on the other hand if it was too low, the free-surface diverged downwards, as shown in Fig.7. Only for a particular value of the coefficient of discharge the free-surface converged to the correct one provided the rough corrections in the θ-distribution are made initially to remove the divergence due to wrong initial assumption.

All the computations were done on the IBM 7044 computer. The large storage required for the ln (V) and θ arrays eliminates the use of small computers.

For all integrations, Simpson's rule and half-Simpson's rule (Ref. 9) were used.

Solution has been obtained for a circular crested spillway for head equal to 2.5 D, wherein D is the diameter of the circular crest. The free-surface and flownet obtained are shown in Fig. 8 and the pressure distribution obtained along the spillway surface is shown in Fig. 9. Twenty one streamlines and ninety equipotential lines were chosen for computation.

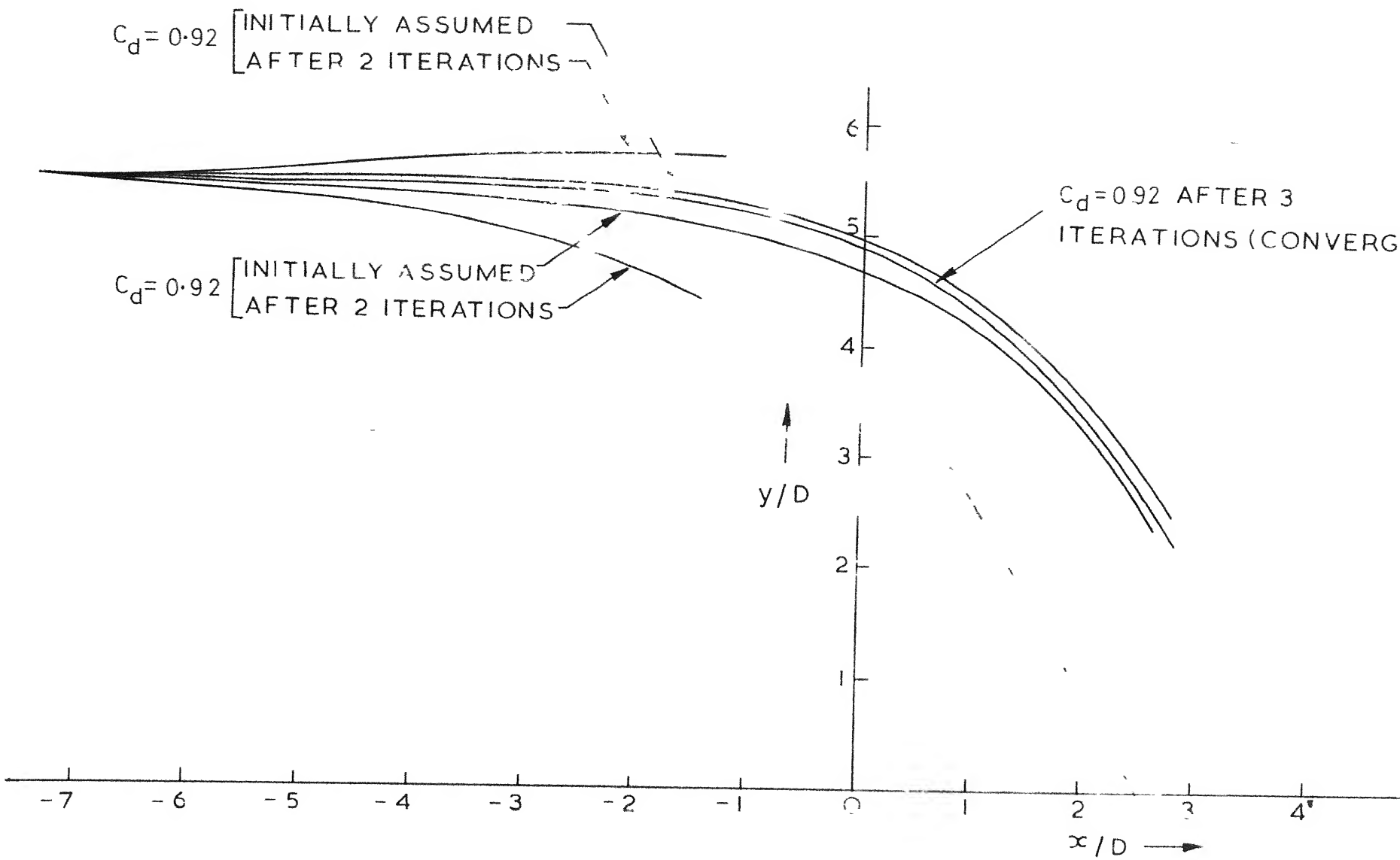

FIG. 6 BEHAVIOR OF FREE-SURFACE-PROFILE FOR DIFFERENT INITIAL ASSUMPTIONS OF FREE SURFACE

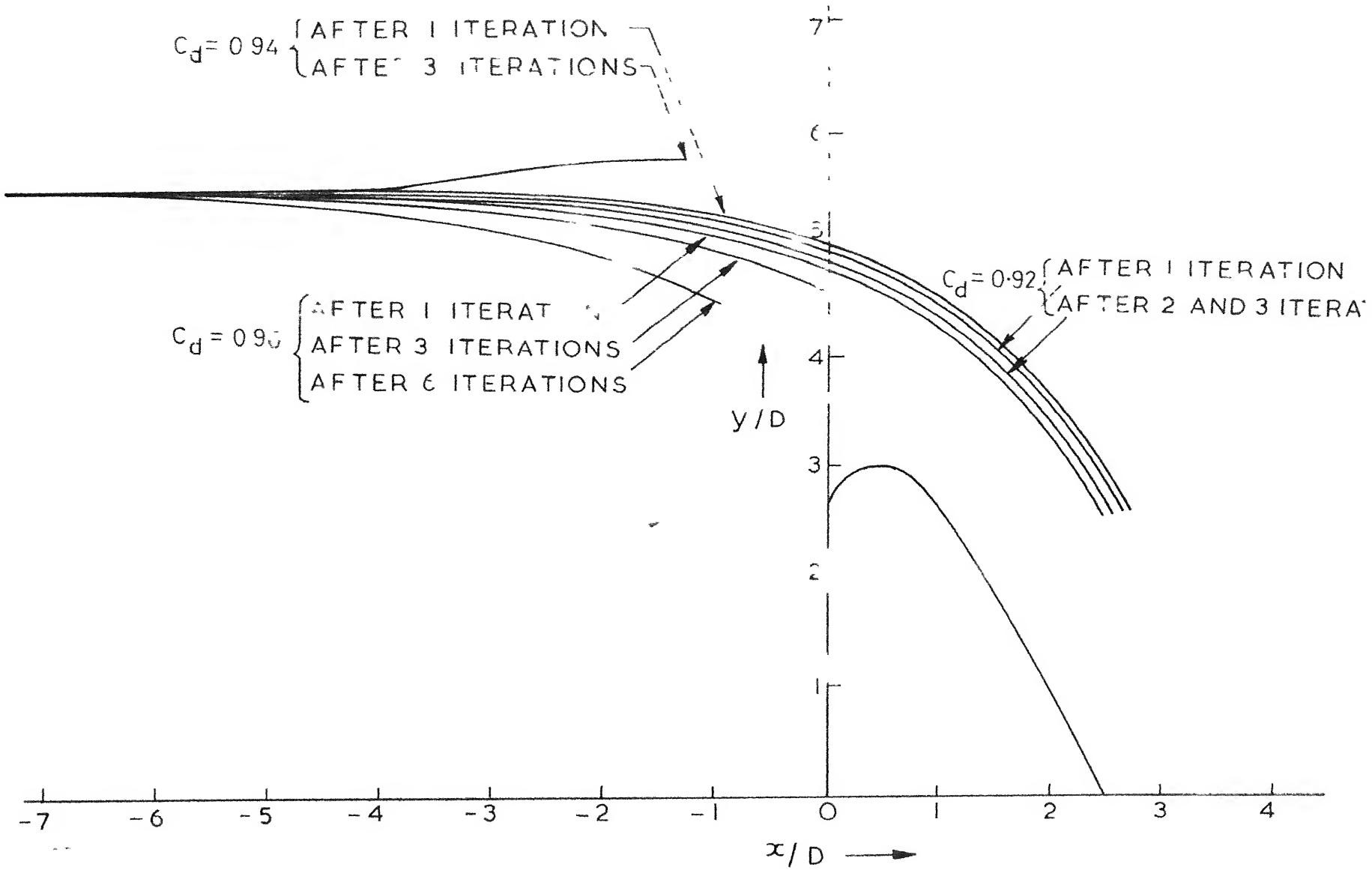

FIG. 7 BEHAVIOR OF FREE-SURFACE-PROFILE FOR DIFFERENT VALUES OF COEFFICIENT OF DISCHARGE

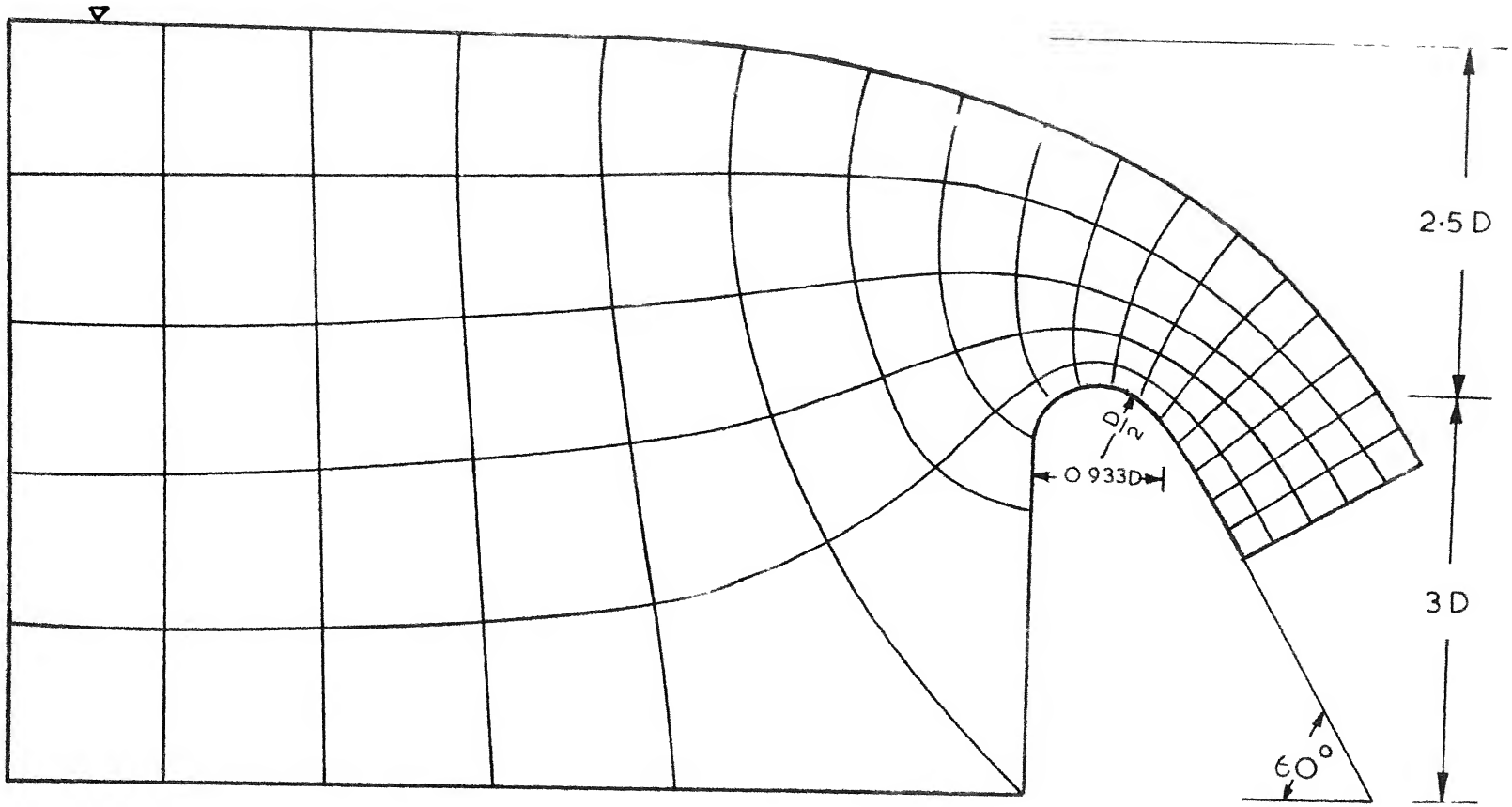

FIG. 8 FREE-SURFACE-PROFILE AND FLOW-NET FOR SPILLWAY WITH CIRCULAR CREST

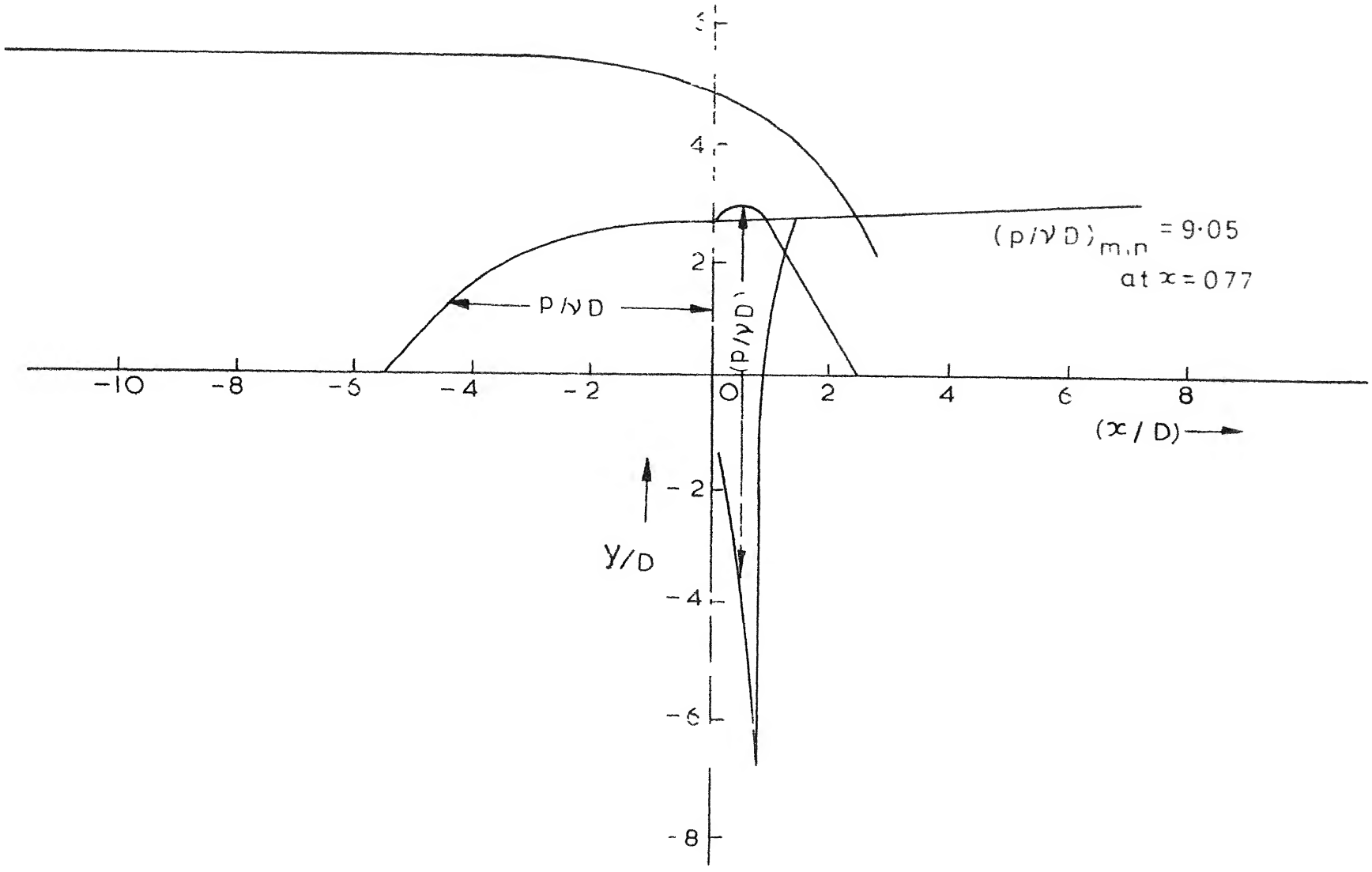

FIG 9 PRESSURE DISTRIBUTION ALONG THE SURFACE OF CIRCULAR CRESTED SPILLWAY FOR $h/D = 2{\cdot}5$

CHAPTER 4

DISCUSSION OF RESULTS AND CONCLUSIONS

4.1 Discussion:

Cassidy has shown that the divergence of the free-surface depends only upon the value of coefficient of discharge. But the present study has shown that the divergence of the free surface, as reported by Cassidy, depends both upon the initial assumed free surface as well as the value of C_d. The divergence was found to be dependent on the value of C_d alone only for a few initially assumed free-surfaces and such a free surface could beobtained after a few trials. Thus the method has not been found to be a simple method of successive approximations but involving trial and error procedure also.

In the procedure suggested by Cassidy, the velocity distribution along the free-surface is obtained directly from the values of y obtained at the end of the previous iteration by using the Bernoulli equation. So, if a free-surface higher than the correct free-surface is assumed, a low velocity distribution throughout the field is obtained for a particular value of coefficient of discharge. This results in higher values of y for the free surface if the integration for y is done along the equipotential line starting from the solid boundary. Thus if

the initially assumed free-surface is higher than the correct free-surface, it becomes still higher and similarly if the initially assumed free-surface is lower than the correct free-surface it becomes still lower after each iteration, even if the correct value is assumed for the coefficient of discharge. On the other hand, if the integration for y is started from the upstream boundary, the behavior of free surface can never be in agreement with what Cassidy has shown. In this case, no algorithm for correcting either the initially assumed free-surface or the value of C_d is obtained.

The behavior of the free-surface profile in the region upstream from the spillway obtained after each iteration using this method becomes erratic particularly due to the fact that even slightest error in the initially assumed ordinates of the free-surface results in error in the velocity distribution along the free-surface upstream from the spillway which is computed directly using Bernoulli equation. When y is computed for the free-surface by integrating along the equipotential line commencing from the solid boundary the error in y is magnified in the region upstream from the spillway as the velocity head is very low in that region as compared to the head.

For the solid boundary, in Cassidy's method, $x(\phi, \psi)$ is computed by using Eqn. 37 and y and θ are then computed by using the equation for the profile of the spillway. This has

the great draw back that the number of equipotential lines joining the vertical face of spillway remains same after each iteration as assumed previously because Δx always remains zero for vertical face and is not corrected after any iteration if the initial assumption is wrong.

Cassidy assumes a mapping function for the corner flow independent of the exterior flow, which does not seem reasonable. But in the present case the mapping function for the corner flow has been obtained from the condition that along a reasonably chosen boundary enclosing the corner, the mapping function and the exterior flow equations should give the same results. The accuracy of such an assumption may be verified by bringing the boundary closer to the corner and observing that there is no change in the results.

In the method developed and presented in the previous chapter, all these drawbacks have been removed. The behavior of free-surface profile remains more stable and the behavior is not erratic so that the algorithm for the correction of the value of C_d may be used easily.

4.2 Conclusions:

In the present study, a method has been developed for the numerical solution of irrotational flow over spillways of finite height. A full study of the method suggested for the same by Cassidy has been conducted and the drawbacks found in

that method have been rectified. The method of solution has been found to be one involving trial and error.

The chief advantage of the method developed herein lies in the fact that there is no erratic behavior of free-surface as seen in the method suggested by Cassidy, if there is any error in the initially assumed free-surface. The solutions obtained after each iteration remain more stable.

The greatest disadvantage of the method is the large computer time required for the relaxation of θ by using equation 34. In the example presented herein, 26 minutes of operational time was taken on IBM 7044 computer for 3 iterations. The time taken depends very much on the number of stream-lines chosen.

The following alternate methods of approach are suggested for future investigations:

1. By using equation 19 instead of equations 21 and 22 for the computation of velocity and using the Cauchy-Reimann equation for θ instead of the Laplace equation the method may be refined and the solution may become more stable (10).

2. Integration for x and y may be carried along the stream lines starting from the downstream boundary also. This may lead to some other divergence-pattern.

3 The effect of the location of upstream and downstream boundary on the results, particularly on the minimum pressure on the surface of the spillway should be investigated.

LIST OF REFERENCES

1. Ippen, A.T., " Channel Transitions and Controls", Engineering Hydraulics, edited by Hunter Rouse, John Wiley and Sons, Inc., New York.

2. Cassidy, J.J., " Designing Spillway Crests for High-Head Operation", Journal of the Hydraulics Division, ASCE, Vol. 96, No. HY3, Proc. paper 7153, March, 1970.

3. Lauck, A., " Ueberfall uber ein Wehr," Zeitschrift fur Angewandte Mathematik und Mechanik, Akademie-Verlag GMBH, Berlin, Germany, Vol. 5, 1925.

4. Southwell, R.V. and Vaisey, G. " Relaxation Method Applied to Engineering Problems. XII Fluid Motions Characterised by 'Free' Stream-lines", Philosophical Transactions, Series A, Vol. 240, 1946.

5. Strelkoff, T.S., " Solution of Highly Curvilinear Gravity Flows," Journal of the Engineering Mechanics Division, ASCE, Vol. 90, No. EM3, Proc. paper 3950, June, 1964.

6. Watters, G., and Streets, R.L., " Two-Dimensional Flow Over Sills in Open Channels", Journal of the Hydraulics Division, ASCE, Vol.90, No. HY4, Proc. paper 3967, July, 1964.

7. Cassidy, John J., " Irrotational Flow Over Spillways of Finite Height," Journal of the Engineering Mechanics Division, ASCE, Vol. 91, No. EM6, Proc. paper 4591, December, 1965.

8. Bickley, W.G., " Finite-Difference Formulae for the Square Lattice," Quarterly Journal of Mechanics and Applied Mathematics, London, England, Vol. 1, Part 1, 1948.

9. McCormick M. and Salvadori Mario G., Numerical Methods in FORTRAN, Prentice-Hall of India Limited, New Delhi, 1968.

10. Lenau, Charles W. and Cassidy J.J., " Flow Through Spillway Flip Bucket" Journal of the Hydraulics Division, ASCE, Vol. 95, No. HY2, March, 1969.

11. Rouse, Hunter, " Elementary Mechanics of Fluids," John Wiley and Sons, New York, N.Y., 1946.

APPENDIX

LISTING OF COMPUTER PROGRAMME

DESCRIPTION OF VARIABLES

CD	=	coefficient of discharge
H	=	head over the spillway crest
HD	=	parameter D as described in chapter 2
I	=	Subscript used to denote equipotential lines (I = 1 refers to the upstream boundary and I = NF refers to the downstream boundary)
ITEST	=	an index (data for ITEST is taken as positive when integration for y is carried only along the equipotential line and ITEST is taken as negative when integration is carried through the two different paths as described in chapter 3.)
J	=	subscript used to denote stream lines. (J = 1 refers to the free surface and J = NS refers to the solid boundary)
MAXIT	=	maximum number of iterations for the relaxation of Θ
NF	=	total number of equipotential lines.
NS	=	number of stream lines
NFIMID	=	value of I for $\emptyset$ = 0 line
NFC	=	number of equipotential lines corresponding to the finer grid near the corner

NSC	=	number of stream lines corresponding to the finer grid near the corner
NFCMID	=	value of I for Ø = 0 line corresponding to the finer grid near the corner
P	=	dimensionless pressure
S	=	Distance along the surface of spillway starting from the origin
THITA	=	angle of inclination of velocity vector with x-direction
V	=	magnitude of velocity vector
W	=	height of the spillway
X	=	x co-ordinate
Y	=	y co-ordinate

LISTING OF PROGRAMME

```
$IBJOB
$IBFTC  MAIN
      DIMENSION  THITA(140,21),STHITA(100,21),VLOG(100,21),V(140,21),X
     140,21),Y(140,21),DUMX(140,2),DUMY(140,2),THITAS(140,2),YS(140),S
     140),THITAC(21,11),VC(11),VLOGC(11),XC(11),YC(11),STHITC(21,11)
      DIMENSION P(140)
      READ 1,NF,NS,NFIMID,MAXIT,MIT,ITEST
      READ 1,NSC,NFC,NFCMID
      COMMON  THITA,X,Y,NS,NF
      COMMON  THITAM
      COMMON  NFIMID
      COMMON HD
      CALL FLUN(500)
      CALL FLOV(500)
      NCHPNT=1
      READ 2,W,H,HD
C     W=W/HD,H=H/HD,HT=HT/HD
      READ 3,CHECKT,CHECKX,CHECKY,CD,CDI,CHECKV
    3 FORMAT(8F10.8)
      THITAM=-ATAN(1.)*4./3.
      PI=ATAN(1.)*4.
C     THITAM=THITA AT D/S END
      NS1=NS-1
      NF1=NF-1
      FIMID=NFIMID
      FNS=NS
      FNS1=NS1
      FNF=NF
      FNSC=NSC
      FNFC=NFC
      FCMID=NFCMID
      FNSC1=NSC-1
      NFC1=NFC-1
      NSC1=NSC-1
C      MAPPING  FUNCTION  W=A*Z**2
      DO 11I=1,NF
      DUMX(I,1)=0.
      DUMX(I,2)=0.
      DUMY(I,1)=0.
      DUMY(I,2)=0.
      DO 11J=1,NS
      STHITA(I,J)=0.
      THITA(I,J)=0.
   11 CONTINUE
      DO 413 I=1,NFC
```

```
      DO 413 J=1,NSC
      THITAC(I,J)=0.
  413 STHITC(I,J)=0.
      CALL          INPUT(Y,THITA,S,NF,NM1,NP1,H,W,THITAM,NFIMID,NS)
      CALL          BOUND(X,Y,THITA,S,NFIMID,NF,NS,THITAM)
      PRINT 7,(X(I,NS),Y(I,NS),I=1,NF)
      K=0
      DO 12 J=1,NS,NS1
      K=K+1
      DO 12 I=1,NF
   12 THITAS(I,K)=THITA(I,J)
      DO 13 I=1,NF
   13 YS(I)=Y(I,1)
  320 CONTINUE
      IFIRST=1
      K=0
      DO 14 J=1,NS,NS1
      K=K+1
      DO 14 I=1,NF
   14 THITA(I,J)=THITAS(I,K)
      DO 15I=1,NF
   15 Y(I,1)=YS(I)
  300 CONTINUE
      Q=(2./3.)*CD*(H**1.5)
      HT=H+W+(Q/(H+W))**2
C     Q IS IN DIMENSIONLESS FORM
      DP1=Q/(FNS-1.)
      DP2=DP1*2.
      DM1=-DP1
      DM2=-DP2
      DP1C=DP1/FNSC1
      DP2C=DP2/FNSC1
      DM1C=DM1/FNSC1
      DM2C=DM2/FNSC1
      PRINT7,DP1,DM2,DP1C,DM2C
      IP1=NFIMID+1
      IM1=NFIMID-1
C     RELAXATION METHOD FOR THITAS
C     THITA FOR CORNER
      THITAC(NFCMID,NSC-1)=PI/4.
      SINE=-1.
      ICM=NFCMID-1
      ICP=NFCMID+1
      DO 54 I=ICM,ICP,2
      FI=SINE*DP1C
```

```
      THITA(NFIMID-1,NS)=0.
      THITA(NFIMID+1,NS)=PI/2.
  281 CONTINUE
      DO 330 ITN=1,NIT
      DO 70 IT=1,MAXIT
      THITA(NFIMID-1,NS1)=(THITA(NFIMID,NS1)+THITA(NFIMID-2,NS1)+THIT
     1FIMID-1,NS)+THITA(NFIMID-1,NS-2))/4.
      THITAC(1,1)=THITA(NFIMID-1,NS1)
      THITA(NFIMID+1,NS1)=(THITA(NFIMID+2,NS1)+THITA(NFIMID+1,NS-2)+TH
     1A(NFIMID,NS1)+THITA(NFIMID+1,NS))/4.
      THITAC(NFC,1)=THITA(NFIMID+1,NS1)
      THITA(NFIMID,NS1)=(THITA(NFIMID+1,NS1)+THITA(NFIMID,NS-2)+THITA
     1IMID-1,NS1)+THITAC(NFCMID,2)*FNSC1)/(3.+FNSC1)
      THITAC(NFCMID,1)=THITA(NFIMID,NS1)
      THITAC(1,NSC)=THITA(NFIMID-1,NS)
      THITAC(NFC,NSC)=THITA(NFIMID+1,NS)
      DO 51 I=2,NFCMID
      THITAC(I,1)=THITAC(I-1,1)+(THITAC(NFCMID,1)-THITAC(1,1))/FNSC1
   51 THITAC(I,NSC)=THITAC(1,NSC)
      I1=NFCMID+1
      DO 52 I=I1,NFC
      THITAC(I,1)=THITAC(I-1,1)+(THITAC(NFC,1)-THITAC(NFCMID,1))/FNSC1
   52 THITAC(I,NSC)=THITAC(NFC,NSC)
      DO 53 J=2,NSC
      THITAC(1,J)=THITAC(1,J-1)+(THITAC(1,NSC)-THITAC(1,1))/FNSC1
   53 THITAC(NFC,J)=THITAC(NFC,J-1)+(THITAC(NFC,NSC)-THITAC(NFC,1))/FN
     11
      DO 50 J=2,NS1
      DO 60 I=2,NF1
      IF(J-NS1)61,62,61
   62 IF(I-IM1)63,60,63
   63 IF(I-NFIMID)64,60,64
   64 IF(I-IP1)61,60,61
   61 CONTINUE
       SUM1=THITA(I,J-1)+THITA(I,J+1)+THITA(I-1,J)+THITA(I+1,J)
      SUM2=THITA(I+1,J+1)+THITA(I+1,J-1)+THITA(I-1,J+1)+THITA(I-1,J-1)
      THITA(I,J)=(4.*SUM1+SUM2)/20.
   60 CONTINUE
   50 CONTINUE
      SI=DP1C
      EX=-FI+(FI**2+SI**2)**0.5
      DYDX=SI/EX
      THITAC(I,NSC-1)=ATAN(DYDX)
      SINE=-SINE
   54 CONTINUE
```

```
      DO450 J=2,NSC1
      DO 460 I=2,NFC1
      IF(J-NSC1)461,462,461
  462 IF(I-ICM)463,460,463
  463 IF(I-NFCMID)464,460,464
  464 IF(I-ICP)461,460,461
  461 CONTINUE
      SUM1=THITAC(I,J-1)+THITAC(I,J+1)+THITAC(I-1,J)+THITAC(I+1,J)
      SUM2=THITAC(I+1,J+1)+THITAC(I+1,J-1)+THITAC(I-1,J+1)+THITAC(I-1
     11)
      THITAC(I,J)=(4.*SUM1+SUM2)/20.
  460 CONTINUE
  450 CONTINUE
      DO 80 I=2,NF1
      DO 80 J=2,NS1
      DIFFT=(STHITA(I,J)-THITA(I,J))/THITA(I,J)
      ERRT=ABS(DIFFT)
      IF(ERRT-CHECKT)80,90,90
   80 CONTINUE
      DO 480 I=2,NFC1
      DO 480 J=2,NSC1
      DIFFT=(STHITC(I,J)-THITAC(I,J))/THITAC(I,J)
      ERRT=ABS(DIFFT)
      IF(ERRT-CHECKT)480,490,490
  480 CONTINUE
      GO TO 110
  490 CONTINUE
   90 CONTINUE
      DO 100 I=1,NF
      DO 100 J=1,NS
  100 STHITA(I,J)=THITA(I,J)
      DO 500 I=1,NFC
      DO 500J=1,NSC
  500 STHITC(I,J)=THITAC(I,J)
   70 CONTINUE
  110 CONTINUE
C     COMPUTATION OF LOG OF V
      CALL          FRISUR(Y,THITA,V,HT,DP1,CHECKV,NF)
      J=1
      DO 120 I=1,NF
      D20=HT-Y(I,J)
      IF(D20)290,111,111
  111 V(I,J)=D20**0.5
      VLOG(I,J)=ALOG(V(I,J))
  120 CONTINUE
```

```
      UVEL=Q/(H+W)
      I=1
      DO 121 J=1,NS
      V(I,J)=UVEL
  121 VLOG(I,J)=ALOG(V(I,J))
      CALL  VELFI(THITA,VLOG,NF,NS,NFIMID,NF1,NS1,DP1,DP2,DM1,DM2,PI)
      VLOGC(1)=VLOG(NFIMID,NS1)
      I=NFCMID
      J=2
      D1=(THITAC(I+1,J-1)-THITAC(I-1,J-1))/DP2C
      D3=(THITAC(I+1,J+1)-THITAC(I-1,J+1))/DP2C
      D2=(THITAC(I+1,J)-THITAC(I-1,J))/DP2C
      DVLOGC=(5.*D1+8.*D2-D3)*DM1C/12.
      VLOGC(J)=VLOGC(J-1)+DVLOGC
      DO 510 J=3,NSC
      D1=(THITAC(I+1,J-2)-THITAC(I-1,J-2))/DP2C
      D2=(THITAC(I+1,J-1)-THITAC(I-1,J-1))/DP2C
      D3=(THITAC(I+1,J)-THITAC(I-1,J))/DP2C
      DVLOGC=(D1+4.*D2+D3)*DM1C/3.
  510 VLOGC(J)=VLOGC(J-2)+DVLOGC
      DO 145 I=1,NF
      DO 145 J=1,NS
  145 V(I,J)=EXP(VLOG(I,J))
      DO 545 I=1,NSC
  545 VC(I)=EXP(VLOGC(I))
      A=(VC(NSC1)**2)/(4.*DP1C)
      PRINT7,A
C     COMPUTATION OF X  AND Y NEAR CORNER
      XC(NSC1)=-(DP1C/(2.*A))**0.5
      YC(NSC1)=-XC(NSC1)
      I=NFCMID
      J=NSC-2
      D1=-SIN(THITAC(I,J+1))/VC(J+1)
      D3=-SIN(THITAC(I,J-1))/VC(J-1)
      D2=-SIN(THITAC(I,J))/VC(J)
      DX=(5.*D1+8.*D2-D3)*DP1C/12.
      XC(J)=XC(J+1)+DX
      D1=COS(THITAC(I,J+1))/VC(J+1)
      D3=COS(THITAC(I,J-1))/VC(J-1)
      D2=COS(THITAC(I,J))/VC(J)
      DY=(5.*D1+8.*D2-D3)*DP1C/12.
      YC(J)=YC(J+1)+DY
      DO 550 K=3,NSC1
      J=NSC-K
      D1=-SIN(THITAC(NFCMID,J))/VC(J)
```

```
      D2=-SIN(THITAC(NFCMID,J+1))/VC(J+1)
      D3=-SIN(THITAC(I,J+2))/VC(J+2)
      DX=(D1+4.*D2+D3)*DP1C/3.
      XC(J)=XC(J+2)+DX
      D3=COS(THITAC(NFCMID,J))/VC(J)
      D4=COS(THITAC(NFCMID,J+1))/VC(J+1)
      D5=COS(THITAC(I,J+2))/VC(J+2)
      DY=(D3+4.*D4+D5)*DP1C/3.
      YC(J)=YC(J+2)+DY
  550 CONTINUE
      X(NFIMID,NS1)=XC(1)
      Y(NFIMID,NS1)=YC(1)
      X(NFIMID+1,NS)=0.
      Y(NFIMID-1,NS)=0.
      PRINT 7,X(NFIMID,NS1),Y(NFIMID,NS1)
      PRINT 7,(XC(J),J=1,NSC)
      PRINT 7,(YC(J),J=1,NSC)
      PRINT 7,(VC(J),J=1,NSC)
      CALL          XYCOMP(X,Y,THITA,V,S,NF,NS,NF1,NS1,NFIMID,DP1,DM1,DP
     1DM2,IFIRST,ITEST,H,W)
      PRINT 7,(X(I,NS),Y(I,NS),I=1,NF)
      CALL  BOUND(X,Y,THITA,S,NFIMID,NF,NS,THITAM)
      K=0
      DO 200 J=1,NS,NS1
      K=K+1
      DO 200 I=1,NF
      IST1=I
      DIFFX=(DUMX(I,K)-X(I,J))/HT
      DIFFY=(DUMY(I,K)-Y(I,J))/HT
      ERRX=ABS(DIFFX)
      ERRY=ABS(DIFFY)
      IF(ERRX-CHECKX)205,210,210
  205 IF(ERRY-CHECKY)200,210,210
  200 CONTINUE
      GO TO 310
  210 CONTINUE
      DO 230 I=1,NF
      DUMX(I,1)=X(I,1)
      DUMY(I,1)=Y(I,1)
      DUMX(I,2)=X(I,NS)
  230 DUMY(I,2)=Y(I,NS)
C     COMPUTAYION OF NEW THITAS
      J=1
      DO 241 I=2,NF1
  240 THITA(I,J)=ATAN((Y(I+1,J)-Y(I-1,J))/(X(I+1,J)-X(I-1,J)))
```

```
241 CONTINUE
246 I=1
    DO 256 J=1,NS1
250 THITA(I,J)=0.
256 CONTINUE
    I=NF
    DO 266 J=1,NS1
260 THITA(I,J)=THITAM
266 CONTINUE
    PRINT 6,IT,IST1,CD
    PRINT 7,(X(I,1),Y(I,1),I=1,NF)
    PRINT 7,(X(I,NS),Y(I,NS),I=1,NF)
    PRINT 7,(THITA(I,1),I=1,NF)
    PRINT 7,(THITA(I,NS),I=1,NF)
330 CONTINUE
    PRINT 7,((X(I,J),Y(I,J),I=1,NF),J=1,NS)
    J=NS
    DO 340 I=IP1,NF
    P(I)=HT-V(I,J)**2-Y(I,J)
    PRINT 6,I,J,X(I,J),Y(I,J),V(I,J),P(I)
340 CONTINUE
    DO 350 I=IP1,NF
    VD=DP2/(S(I+1)-S(I-1))
    ER=(V(I,J)-VD)/V(I,J)
    PRINT 6,I,J,V(I,J),VD,ER
350 CONTINUE
    J=1
    DO 360 I=1,NF
    P(I)=HT-V(I,J)**2-Y(I,J)
    PRINT 7,P(I)
360 CONTINUE
    CALL        XYCOMP(X,Y,THITA,V,S,NF,NS,NF1,NS1,NFIMID,DP1,DM1,DP
   1DM2,IFIRST,ITEST,H,W)
    GO TO 281
280 CONTINUE
290 CD=CD+CDI
    GO TO 320
  1 FORMAT(20I3)
  2 FORMAT(8F10.5)
  6 FORMAT(2I5,4E15.7)
  7 FORMAT(10E13.5)
  8 FORMAT(8F15.6)
  9 FORMAT(6F13.5)
600 FORMAT(10F8.5)
310 CONTINUE
    STOP
    END
```

```
$IBFTC  VELFI
      SUBROUTINE  VELFI(THITA,VLOG,NF,NS,NFIMID,NF1,NS1,DP1,DP2,DM1,
     1PI)
      DIMENSION  THITA(140,21),VLOG(100,21)
      IM1=NFIMID-1
      IP1=NFIMID+1
      DO 400 I=2,NF1
      DO 400 J=2,NS
      IF(J-2)20,10,20
   10 D1=(THITA(I+1,J-1)-THITA(I-1,J-1))/DP2
      D3=(THITA(I+1,J+1)-THITA(I-1,J+1))/DP2
      D2=(THITA(I+1,J)-THITA(I-1,J))/DP2
      DVLOG=(5.*D1+8.*D2-D3)*DM1/12.
      VLOG(I,J)=VLOG(I,J-1)+DVLOG
   13 IF(I-2)11,12,11
   12 D1=0.
      D2=-(THITA(I,J+1)-THITA(I,J-1))/DM2
      D3=-(THITA(I+1,J+1)-THITA(I+1,J-1))/DM2
   31 D=(5.*D1+8.*D2-D3)*DP1/12.
      VLOG(I,J)=(VLOG(I,J)+VLOG(I-1,J)+D)/2.
      GO TO 400
   11 D1=-(THITA(I-2,J+1)-THITA(I-2,J-1))/DM2
      D2=-(THITA(I-1,J+1)-THITA(I-1,J-1))/DM2
      D3=-(THITA(I,J+1)-THITA(I,J-1))/DM2
   32 D=(D1+4.*D2+D3)*DP1/3.
      VLOG(I,J)=(VLOG(I,J)+VLOG(I-2,J)+D)/2.
      GO TO 400
   20 IF(J-NS)60,70,60
   60 D1=(THITA(I+1,J-2)-THITA(I-1,J-2))/DP2
      D2=(THITA(I+1,J-1)-THITA(I-1,J-1))/DP2
      D3=(THITA(I+1,J)-THITA(I-1,J))/DP2
      GO TO 300
   70 IF(I-NFIMID)80,90,80
   90 GO TO 400
   80 IF(I-IM1)100,110,100
  110 D1=(THITA(I+1,J-2)-THITA(I-1,J-2))/DP2
      D2=(THITA(I+1,J-1)-THITA(I-1,J-1))/DP2
      D3=0.
      GO TO 300
  100 IF(I-IP1)60,110,60
  300 DVLOG=(D1+4.*D2+D3)*DM1/3.
      VLOG(I,J)=VLOG(I,J-2)+DVLOG
      IF(J-NS1)14,15,14
   15 IF(I-NFIMID)17,16,17
   16 THITA(I,J+1)=PI/4.
```

```
      GO TO 11
17    IF(I-IP1)18,19,18
19    THITA(I-1,J+1)=PI/4.
      GO TO 11
18    IF(I-IP1-1)13,33,13
33    THITA(I-2,J+1)=PI/4.
      GO TO 11
14    IF(J-NS)13,21,13
21    IF(I-NFIMID)22,400,22
22    IF(I-IP1)23,400,23
23    IF(I-IP1-1)25,26,25
25    IF(I-2)27,26,27
26    D1=-(THITA(I-1,J)-THITA(I-1,J-1))/DM1
      D3=-(THITA(I+1,J)-THITA(I+1,J-1))/DM1
      D2=-(THITA(I,J)-THITA(I,J-1))/DM1
      GO TO 31
27    D1=-(THITA(I-2,J)-THITA(I-2,J-1))/DM1
      D2=-(THITA(I-1,J)-THITA(I-1,J-1))/DM1
      D3=-(THITA(I,J)-THITA(I,J-1))/DM1
      GO TO 32
400   CONTINUE
      I=NF
      DO 500 J=2,NS
500   VLOG(I,J)=VLOG(I,1)
      RETURN
      END
```

```
$IBFTC  BOUND
      SUBROUTINE  BOUND(X,Y,THITA,S,NFIMID,NF,NS,THITAM)
      DIMENSION X(140,21),Y(140,21),THITA(140,21),S(140)
      J=NS
      PI=ATAN(1.)*4.
      ST1=2.5
      ST2=ST1+PI*5./12.
      XT2=0.5*(1.-COS(PI*5./6.))
      YT2=0.5*SIN(PI*5./6.)+ST1
      DO 100I=NFIMID,NF
      IF(S(I)-ST1)10,10,20
   10 THITA(I,J)=PI/2.
      X(I,J)=0.
      Y(I,J)=S(I)
      GO TO 100
   20 IF(S(I)-ST2)30,30,40
   30 THITA(I,J)=5.+PI/2.-S(I)*2.
      ALFA=PI/2.-THITA(I,J)
      X(I,J)=0.5*(1.-COS(ALFA))
      Y(I,J)=0.5*SIN(ALFA)+ST1
      GO TO 100
   40 THITA(I,J)=-PI/3.
      X(I,J)=XT2+(S(I)-ST2)*COS(-THITAM)
      Y(I,J)=YT2-(S(I)-ST2)*SIN(-THITAM)
  100 CONTINUE
    1 FORMAT(9F12.5)
      RETURN
      END
$IBFTC  FRISUP
      SUBROUTINE  FRISUP(Y,THITA,V,HT,DP1,CHECKV,NF)
      DIMENSION  Y(140,21),THITA(140,21),V(140,21)
      J=1
      I=2
   10 YP=Y(I,J)
      V(I,J)=(HT-Y(I,J))**0.5
      D1=SIN(THITA(I-1,J))/V(I-1,J)
      D2=SIN(THITA(I,J))/V(I,J)
      DY=(D1+D2)*DP1/2.
      Y(I,J)=Y(I-1,J)+DY
      ER=ABS(YP-Y(I,J))
      ERMAX=(HT-Y(I,J))*CHECKV
      IF(ER-ERMAX)20,20,10
   20 CONT+NUE
      DO 30 I=3,NF
   40 YP=Y(I,J)
```

```
      V(I,J)=(HT-Y(I,J))**0.5
      D1=SIN(THITA(I-2,J))/V(I-2,J)
      D2=SIN(THITA(I-1,J))/V(I-1,J)
      D3=SIN(THITA(I,J))/V(I,J)
      DY=(D1+4.*D2+D3)*DP1/3.
      Y(I,J)=Y(I-2,J)+DY
      ER=ABS(YP-Y(I,J))
      ERMAX=(HT-Y(I,J))*CHECKV
      IF(ER-ERMAX)30,30,40
30    CONTINUE
      PRINT 7,(Y(I,J),I=1,NF)
 7    FORMAT(10E12.5)
      RETURN
      END
```

```
$IBFTC  XYCOMP
       SUBROUTINE  XYCOMP(X,Y,THITA,V,S,NF,NS,NF1,NS1,NFIMID,DP1,DM1,DP
      1DM2,IFIRST,ITEST,H,W)
       DIMENSION X(140,21),Y(140,21),THITA(140,21),V(140,21),S(140)
       FNF=NF
       FNF1=NF1
       FNS=NS
       FNS1=NS1
       I=NFIMID-1
       J=NS1
       D1=COS(THITA(I+1,J))/V(I+1,J)
       D2=COS(THITA(I,J))/V(I,J)
       D3=COS(THITA(I-1,J))/V(I-1,J)
       D=(5.*D1+8.*D2-D3)*DP1/12.
       X(I,J)=X(I+1,J)-D
       J=NS
       D1=-SIN(THITA(I,J-2))/V(I,J-2)
       D2=-SIN(THITA(I,J-1))/V(I,J-1)
       D3=-SIN(THITA(I,J))/V(I,J)
       D=(-D1+8.*D2+5.*D3)*DP1/12.
       Y(I,J)=X(I,J-1)-D
       I=NFIMID+1
       J=NS1
       D1=SIN(THITA(I-1,J))/V(I-1,J)
       D2=SIN(THITA(I,J))/V(I,J)
       D3=SIN(THITA(I+1,J))/V(I+1,J)
       D=(5.*D1+8.*D2-D3)*DP1/12.
       Y(I,J)=Y(I-1,J)+D
       J=NS
       D1=COS(THITA(I,J-2))/V(I,J-2)
       D2=COS(THITA(I,J-1))/V(I,J-1)
       D3=COS(THITA(I,J))/V(I,J)
       D=(-D1+8.*D2+5.*D3)*DP1/12.
       S(I)=Y(I,J-1)-D
       I=NFIMID
       J=NS-2
       D1=-SIN(THITA(I,J+1))/V(I,J+1)
       D3=-SIN(THITA(I,J-1))/V(I,J-1)
       D2=-SIN(THITA(I,J))/V(I,J)
       D=(5.*D1+8.*D2-D3)*DP1/12.
       X(I,J)=X(I,J+1)+D
       D1=COS(THITA(I,J+1))/V(I,J+1)
       D3=COS(THITA(I,J-1))/V(I,J-1)
       D2=COS(THITA(I,J))/V(I,J)
       D=(5.*D1+8.*D2-D3)*DP1/12.
```

```
      Y(I,J)=Y(I,J+1)+D
      I=NFIMID-2
      J=NS
      D1=COS(THITA(I+1,J))/V(I+1,J)
      D3=COS(THITA(I-1,J))/V(I-1,J)
      D2=COS(THITA(I,J))/V(I,J)
      D=(5.*D1+8.*D2-D3)*DP1/12.
      X(I,J)=X(I+1,J)-D
      Y(I,J)=0.
      I=NFIMID+2
      D1=SIN(THITA(I-1,J))/V(I-1,J)
      D3=SIN(THITA(I+1,J))/V(I+1,J)
      D2=SIN(THITA(I,J))/V(I,J)
      D=(5.*D1+8.*D2-D3)*DP1/12.
      S(I)=S(I-1)+D
      X(I,J)=0.
      J=NS
      I2=NFIMID-1
      DO 150 K=3,I2
      I=NFIMID-K
      Y(I,J)=0.
      D1=1./V(I+2,J)
      D2=1./V(I+1,J)
      D3=1./V(I,J)
      D=(D1+4.*D2+D3)*DP1/3.
  150 X(I,J)=X(I+2,J)-D
      I=1
      DO 161 J=1,NS
      FJ=J
      X(I,J)=X(1,NS)
  161 Y(I,J)=(H+W)*(FNS-FJ)/FNS1
      I=2
      DO 155 K=1,NS1
      J=NS-K
      IF(J-NS1)152,151,152
  151 CONTINUE
      D1=-SIN(THITA(I,J+1))/V(I,J+1)
      D3=-SIN(THITA(I,J-1))/V(I,J-1)
      D2=-SIN(THITA(I,J))/V(I,J)
      D=(5.*D1+8.*D2-D3)*DP1/12.
      X(I,J)=X(I,J+1)+D
      D1=COS(THITA(I,J+1))/V(I,J+1)
      D3=COS(THITA(I,J-1))/V(I,J-1)
      D2=COS(THITA(I,J))/V(I,J)
      D=(5.*D1+8.*D2-D3)*DP1/12.
```

```
      Y(I,J)=Y(I,J+1)+D
      GO TO 153
  152 D1=-SIN(THITA(I,J+2))/V(I,J+2)
      D2=-SIN(THITA(I,J+1))/V(I,J+1)
      D3=-SIN(THITA(I,J))/V(I,J)
      D=(D1+4.*D2+D3)*DP1/3.
      X(I,J)=X(I,J+2)+D
      D1=COS(THITA(I,J+2))/V(I,J+2)
      D2=COS(THITA(I,J+1))/V(I,J+1)
      D3=COS(THITA(I,J))/V(I,J)
      D=(D1+4.*D2+D3)*DP1/3.
      Y(I,J)=Y(I,J+2)+D
  153 D1=COS(THITA(I-1,J))/V(I-1,J)
      D3=COS(THITA(I+1,J))/V(I+1,J)
      D2=COS(THITA(I,J))/V(I,J)
      D=(5.*D1+8.*D2-D3)*DP1/12.
      X(I,J)=(X(I-1,J)+D+X(I,J))/2.
      D1=SIN(THITA(I-1,J))/V(I-1,J)
      D3=SIN(THITA(I+1,J))/V(I+1,J)
      D2=SIN(THITA(I,J))/V(I,J)
      D=(5.*D1+8.*D2-D3)*DP1/12.
      Y(I,J)=(Y(I-1,J)+D+Y(I,J))/2.
  155 CONTINUE
      J=NS
      S(NFIMID)=0.
      I3=NFIMID+3
      DO 160 I=I3,NF
      D1=1./V(I-2,J)
      D2=1./V(I-1,J)
      D3=1./V(I,J)
      D=(D1+4.*D2+D3)*DP1/3.
      S(I)=S(I-2)+D
  160 CONTINUE
      NS2=NS-2
      DO 180 K=1,NS1
      DO 180 I=3,NF
      J=NS-K
      IF(J-NS1)176,170,176
  176 IF(J-NS2)171,177,171
  177 IF(I-NFIMID)171,172,171
  170 IF(I-NFIMID)173,172,173
  173 CONTINUE
      D1=-SIN(THITA(I,J+1))/V(I,J+1)
      D3=-SIN(THITA(I,J-1))/V(I,J-1)
      D2=-SIN(THITA(I,J))/V(I,J)
```

```
      D=(5.*D1+8.*D2-D3)*DP1/12.
      X(I,J)=X(I,J+1)+D
      D1=COS(THITA(I,J+1))/V(I,J+1)
      D3=COS(THITA(I,J-1))/V(I,J-1)
      D2=COS(THITA(I,J))/V(I,J)
      D=(5.*D1+8.*D2-D3)*DP1/12.
      Y(I,J)=Y(I,J+1)+D
      GO TO 172
  171 D1=-SIN(THITA(I,J+2))/V(I,J+2)
      D2=-SIN(THITA(I,J+1))/V(I,J+1)
      D3=-SIN(THITA(I,J))/V(I,J)
      D=(D1+4.*D2+D3)*DP1/3.
      X(I,J)=X(I,J+2)+D
      D1=COS(THITA(I,J+2))/V(I,J+2)
      D2=COS(THITA(I,J+1))/V(I,J+1)
      D3=COS(THITA(I,J))/V(I,J)
      D=(D1+4.*D2+D3)*DP1/3.
      Y(I,J)=Y(I,J+2)+D
      IF(ITEST.GT.0) GO TO 180
  172 D1=COS(THITA(I-2,J))/V(I-2,J)
      D2=COS(THITA(I-1,J))/V(I-1,J)
      D3=COS(THITA(I,J))/V(I,J)
      D=(D1+4.*D2+D3)*DP1/3.
      X(I,J)=(X(I,J)+X(I-2,J)+D)/2.
      D1=SIN(THITA(I-2,J))/V(I-2,J)
      D2=SIN(THITA(I-1,J))/V(I-1,J)
      D3=SIN(THITA(I,J))/V(I,J)
      D=(D1+4.*D2+D3)*DP1/3.
      Y(I,J)=(Y(I-2,J)+D+Y(I,J))/2.
  180 CONTINUE
      RETURN
      END
```

```
$IBFTC  INPUT
      SUBROUTINE  INPUT(Y,THITA,S,NF,NM1,NP1,H,W,THITAM,NFIMID,NS)
      DIMENSION  DYDX(100),Y(140,21),THITA(140,21),S(140)
      NM1=NFIMID-1
      NP1=NFIMID+1
      READ 9,N1,FNDEX
    9 FORMAT(I3,5F5.2)
    1 FORMAT(10I3)
      J=1
      N2=N1+1
      READ2,(DYDX(K),K=N2,NF)
    2 FORMAT(8F10.5)
      READ 2,(Y(I,J),I=N2,NF)
      DO 20 I=N2,NF
   20 THITA(I,J)=-ATAN(DYDX(I))
        DO 10 I=1,N1
      FI=I
      FN1=N1
      THITA(I,J)=THITA(N2,J)*(((FI-1.)/FN1)**FNDEX)
   10 Y(I,J)=(H+W)-(H+W-Y(N2,J))*(FI-1.)/FN1
      J=NS
      DO 30 I=1,NM1
   30 THITA(I,J)=0.
      READ 2,(S(I),I=NFIMID,NF)
      I=1
      DO 40 J=1,NS
   40 THITA(I,J)=0.
      I=NF
      DO 50 J=1,NS
   50 THITA(I,J)=THITAM
      PRINT 7,(THITA(I,1),I=1,NF)
      PRINT 7,(Y(I,1),I=1,NF)
    7 FORMAT(10E12.5)
      RETURN
      END
```